ADVANCED 3D FLUOROSCOPIC ANALYSIS OF IMPLANTED JOINTS

M. J. Kuhn, M. R. Mahfouz, B. C. Merkl
Center for Musculoskeletal Research, University of Tennessee, Knoxville, TN, USA
e-mail: mmahfouz@utk.edu

Abstract- **Utilizing fluoroscopy for three-dimensional (3D) *in vivo* analysis is a powerful tool with widespread applications. It allows joints (both implanted and normal) to be studied in vivo under weight bearing conditions through normal day-to-day activities such as walking, leg bending, arm raising, etc. Our robust 3D-to-2D registration method allows 3D data to be extracted more accurately than similar techniques which employ an added preliminary segmentation step. After extracting the 3D data, many different joint-specific 3D analyses can be performed. This includes automatic calculation of hip separation, loci tracking of different joints (e.g. hip, vertebrae, shoulder), automatic tracking of ligament attachments, etc. We have also extended our 3D-to-2D registration method to automatically fit a large number of closely spaced images (e.g. 200-500), which we term "video fitting". This provides smoother motion of the implanted models through a given activity. Also, we are able to calculate the contact area between two models. This provides contact area information over a range of activities for more advanced analysis of the knee joint which could be used as input into a finite element model for further analysis.**
***Keywords* - 3D-2D registration, fluoroscopy, contact area**

I. INTRODUCTION

Fluoroscopy has emerged as a powerful tool for analyzing implanted joints *in vivo*. The ability to capture data dynamically opens up many applications compared to still X-rays. This combined with the freedom of motion allowed by single plane fluoroscopy allows analysis of many weight bearing activities. Komistek et al. have used fluoroscopy to perform many distinct 3D analyses including calculation of *in vivo* loading of the knee joint [1], calculation of hip separation after total hip arthroplasty [2], and performance comparison of posterior stabilized versus posterior cruciate-retaining total knee arthroplasty (TKA) [3]. Work has also been done using this same 3D-to-2D registration technique to analyze normal bones. This includes analysis of normal knees through fluoroscopy [4] as well as *in vivo* analysis of patients with and without anterior cruciate ligaments [5].

The robust 3D-to-2D registration technique utilized in these fluoroscopic analyses is outlined in [6]. As discussed in [7], this direct registration method outperforms similar methods which employ an added segmentation step to extract a contour around the implant from the original fluoro image. Once the 3D information has been extracted from fluoroscopy data, a full 3D analysis of the joint is performed. This includes calculation of hip separation, loci tracking of different joints (e.g. hip, vertebrae, shoulder), and automatic tracking of ligament attachments. Recently another tool has been added, which we term "video fitting". Instead of analyzing a small number of images for a given activity (e.g. capturing a fluoro image every 10° for a deep knee bend (DKB)), the activity is analyzed using a large number of closely spaced images. As outlined in Section II-B, this makes fitting the entire image sequence almost completely automated and also provides significantly more data points in analyzing the activity. Finally, another tool has been added to calculate the contact area for each condyle between the femoral and polyethylene components.

This paper is organized as follows: Section II describes the methodology behind the 3D analysis techniques, Section III presents experimental results obtained from contact area analysis including a comparison of our contact area technique versus actual wear from a polyethylene retrieval, and Section IV discusses and concludes.

II. METHODOLOGY

A. Direct 3D-to-2D registration

The techniques employed in our different analytical tools are tailored to distinct applications and therefore largely vary from one to another. The 3D-to-2D registration method was developed previously [6,7]. A brief overview is provided here as background information for the extension of this method to video fitting. The basic setup used in 3D reconstruction of the fluoroscopy scene is shown in Fig. 1. Details of this method can be found in [6], including optimization techniques used, sensitivity to manual bias determined through range of convergence (ROC) testing, and the process of rendering a 2D image of the implant from its 3D pose, dilating it, and correlating it against the original fluoroscopy image.

Next, Fig. 2 shows a contour that has been manually traced around the femoral implant seen in the fluoroscopy image of Fig. 1. As discussed in [7], many 3D-to-2D registration techniques have been proposed which start by tracing a contour around the implant, similar to the one shown in Fig. 2. After extracting the contour, it is matched either against a template library [8,9] or by measuring the distance between the predicted and actual contours [10]. As discussed in [7], these techniques rely heavily on the segmented contour. Therefore, noise, occlusion, and poorly

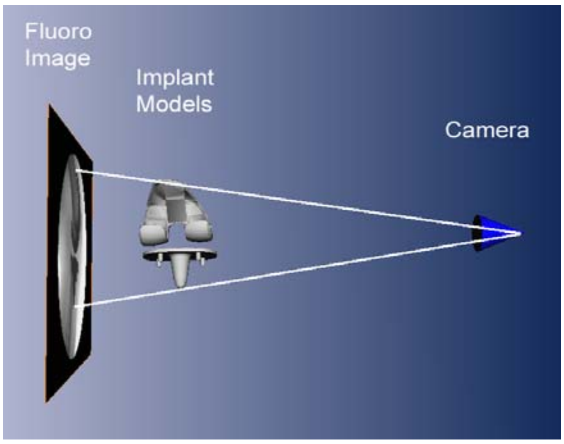

Fig. 1. Layout of 3D scene as viewed by fluoroscopy camera.

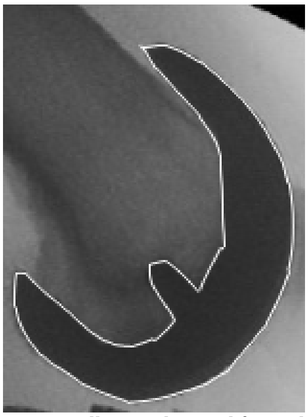

Fig. 2. Contour manually traced around femoral component.

defined edges can largely degrade the performance of these methods. Our direct registration method correlates the predicted image to the original fluoroscopy image, eliminating the need to extract contours around the model silhouette. Consequently, direct registration performs better especially when dealing with noisy or occluded fluoroscopic images [7].

B. Video Fitting

In order to perform the 3D-to-2D registration outlined in Section II-A, a starting pose for each model must be manually specified. When an activity such as a DKB is broken down into 10-15 fluoroscopic images, a starting position is manually specified to fit each image. Video fitting almost completely eliminates this manual dependency by automatically fitting a large sequence of closely spaced images. The user only has to manually provide a starting point for the model close to its correct position for the first image of the sequence. All subsequent images are automatically fit by using the final pose of the previous image as the initial pose for the next image. This concept is illustrated in Fig. 3.

This example exaggerates the differences seen between consecutive images to highlight the video fitting process. The 3D-to-2D registration algorithm outlined in Section II-A is used to fit the 3D models to each fluoroscopy image given a starting pose. The final pose represents the pose which scored the highest using our direct registration method. The

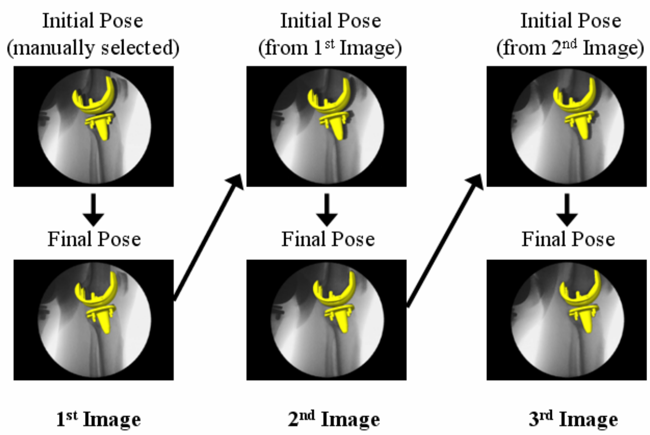

Fig. 3. Exaggerated example of video fitting process.

video fitting process has been run on large image sequences over 200 images. The elimination of user interaction combined with the large amount of data received makes video fitting a useful extension to our basic 3D-to-2D registration method.

C. Contact Area

Another tool added for 3D analysis is automatic calculation of contact area. This is most often used to find the contact area for each femoral condyle with the polyethylene component, although the user interface has been setup to allow contact area to be calculated between two arbitrary models. Fig. 4 shows a fluoroscopic image with the correctly fit femoral, tibial, and polyethylene components. Fig. 5 shows the corresponding distance map and user interface used for contact area calculation.

The polyethylene component in Fig. 4 is rigidly aligned to the top of the tibial component and is transformed to its correct position using the tibial component transformation. A distance map is then generated between the two selected models, as shown in Fig. 5. There can be some slight ambiguity in how “contact” is defined. It is initially defined as distances of +/- 1mm (negative distances indicating intersection of the models). The user interface allows this range to be changed, which is needed in some cases due to the approximation made by rigidly attaching the polyethylene insert to the tibial implant.

III. Results

The tools outlined in Section II are used primarily to obtain results for more clinical-based studies. Given that fact, coherently presenting results for the video fitting and contact area methodologies is somewhat difficult. The contact

Fig. 4. Overlay with polyethylene component inserted.

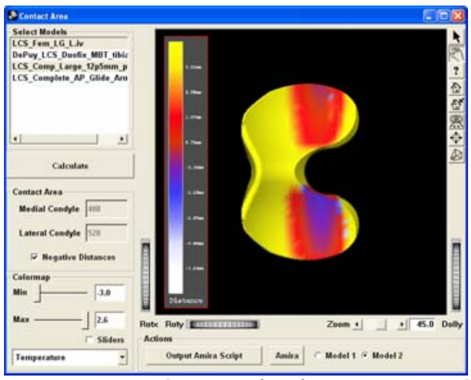

Fig. 5 Distance map and user interface for contact area analysis.

area functionality described in Section II-C was used to calculate wear during DKB and gait activities for a wear retrieval patient. Before undergoing a revision, the patient performed both DKB and gait activities. Fig. 5 shows the contact area averaged over four discrete points along the DKB (0°,30°,60°,70° flexion) as well as the contact area during the heel strike of a gait cycle for a right kneed revision patient. Although there is significant overlap between the contact area during DKB and heel strike, some variation is seen especially on the lateral condyle.

Next, the contact models in Fig. 6 were compared to the retrieval obtained after the patient underwent a revision surgery. Fig. 7a shows the retrieved polyethylene model with noticeable wear on both the medial and lateral condyles. Although wear occurs during both DKB and gait, in normal day-to-day situations gait activities happen substantially more than DKBs. The largest force endured by the knee during gait is at heel strike. Therefore it can be assumed that the wear seen during heel strike should correlate well with the overall wear of the polyethylene component. This claim is validated in Fig. 7b where the contact area shown in Fig. 6 for heel strike is overlayed on the actual polyethylene model shown in Fig. 7a.

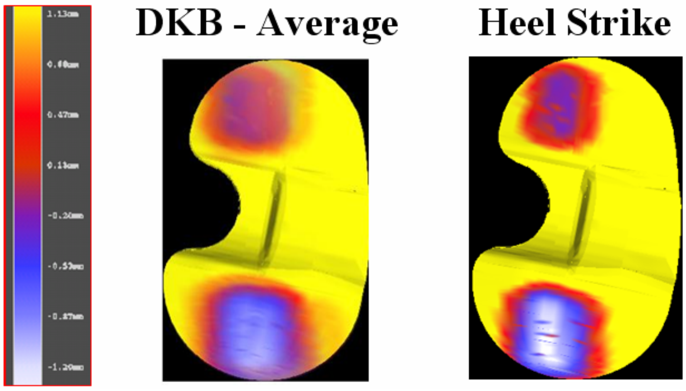

Fig. 6 Contact area averaged over four points along a DKB activity (0°,30°,60°,70° flexion) compared to contact area at the heel strike of a gait cycle for a right kneed revision patient Light areas correspond to -1mm (wear) and dark areas to .5mm (registration limitations) distances.

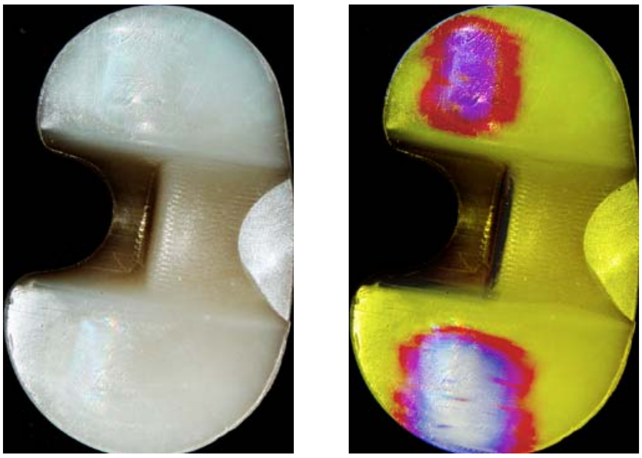

(a) (b)

Fig. 7 – a) Actual polyethylene retrieval b) Average contact area over DKB overlayed on polyethylene retrieval which highlights main regions of wear.

IV. Conclusion

The wear analysis presented in Section III highlights one application of the contact area functionality. In the future this contact information will be used as input for finite element models of the polyethylene. The goal is to do a finite element analysis of patients with a wide variety of implant types to gain a broad knowledge of how the different polyethylene components wear *in vivo*. Although results were not presented for the video fitting, work is currently being done to do a comparison between automated video fitting results and manually specifying the initial pose for each image in a 300 image sequence. The end goal is to show a reduction in error due to the elimination of manual bias. Also, ROC testing was done in [6] on the convergence of the 3D-to-2D registration algorithm. The results show excellent convergence even for initial positions far away from the true pose (16mm in-plane translation, 128mm out-of-plane translation, and 16° of rotation around a randomly directed axis). The maximum displacement of the knee between frames when video is captured at 30 frames/sec for DKB and gait has been within this ROC for all video sequences analyzed, validating use of the final pose from a previous image as the initial pose for the following image.

Fluoroscopy is a powerful tool for analysis of joints during dynamic, weight bearing activities. Two powerful new tools have been introduced that build on our fundamental 3D-to-2D registration method. Video fitting represents the next generation of 3D fluoroscopic analysis and will serve as a useful technique for more advanced 3D analysis techniques of fluoroscopy in the future. Calculation of contact area, combined with finite element methods, opens up new areas of analysis on both wear and the internal stress/strain characteristics of polyethylene components.

References

[1] R. D. Komistek, T. R. Kane, M. R. Mahfouz, J. A. Ochoa and D. A. Dennis, "Knee mechanics: a review of past and present techniques to determine in vivo loads," *J. Biomech.*, 2005, Vol. 2, 215-28.

[2] R. D. Komistek, D. A. Dennis, J. A. Ochoa, B. D. Haas and C. Hammill, "In vivo comparison of hip separation after metal-on-metal or metal-on-polyethylene total hip arthroplasty," *J. Bone Joint Surg.*, 2002, Vol. 10, 1836-41.

[3] R. D. Komistek, R. D. Scott, D. A. Dennis, D. Yasgur, D. T. Anderson and M. E. Hajner, "In vivo comparison of femorotibial contact positions for press-fit posterior stabilized and posterior cruciate-retaining total knee arthroplasties," *J. Arthro.*, 2002, Vol. 2, 209-16.

[4] R. D. Komistek, D. A. Dennis and M. R. Mahfouz, "In vivo fluoroscopic analysis of the normal human knee," *Clin. Orthop.*, 2003, Vol. 410, 69-81.

[5] R. D. Komistek, J. Allain, D. T. Anderson, D. A. Dennis and D. Goutallier, "In vivo kinematics for subjects with and without an anterior cruciate ligament," *Clin. Orthop.*, 2002, Vol. 404, 315-25.

[6] M. R. Mahfouz, W. A. Hoff, R. D. Komistek and D. A. Dennis, "A robust method for registration of three-dimensional knee implant models to two-dimensional

fluoroscopy images," *IEEE Trans. Med. Imag*., 2003, Vol. 12, 1561-74.
[7] M. R. Mahfouz, W. A. Hoff, R. D. Komistek and D. A. Dennis, "Effect of segmentation errors on 3D-to-2D registration of implant models in X-ray images," *J. Biomech*., 2005, Vol. 2, 229-39.
8. S. A. Banks and W. A. Hodge, "Accurate measurement of three-dimensional knee replacement kinematics using single-plane fluoroscopy," *IEEE Trans. Biomed. Engr*., 1996, Vol. 6, 638-49.
[9] W. A. Hoff, R. D. Komistek, D. A. Dennis, S. M. Gabriel and S. A. Walker, "Three-dimensional determination of femoral-tibial contact positions under in-vivo conditions using fluoroscopy," *Clin. Biomech*., Vol. 7, 455-72.
[10] R. Basri and D. Weinshall, "Distance metric between 3D models and 2D images for recognition and classification," *IEEE Trans. Pat. Anal. Mach. Intel*., Vol. 4, 465-79.